

Simulation of Tagger Backgrounds coming from the 12 GeV Electron Beam Halo

Richard Jones, University of Connecticut

February 6, 2007

Abstract

Detailed ray-tracing simulations of the 12 GeV electron beam at the position of the Hall D photon radiator have recently become available. These results make it possible for the first time to estimate the backgrounds in the tagger focal plane that arise from beam particles that are outside the nominal beam envelope. This note describes how a beam halo model was extracted from the accelerator simulation data, and estimates the impact that the expected halo fractions will have on the observed rates in the tagging counters.

In the original report on the electron beam requirements for GlueX [1], a preliminary estimate was made of how much background would be produced in the tagging counters for a given fraction of electron beam particles that fall outside the nominal beam envelope. An upper limit of 10^{-5} for the halo fraction was estimated, based on the criterion that no more than 1% of the rates in the tagging counters should be produced by background coming from halo, where halo was defined to be any particles crossing the plane of the radiator outside a 5σ ellipse around the beam centroid. This estimate was based on the very conservative assumption that halo particles are uniformly distributed over a disk completely filling the 1.5 in. diameter electron beam pipe.

The Jefferson Lab CASA group has recently produced a report describing the detailed shape and momentum profile of the electron beam at the Hall D radiator [2]. The report describes a detailed Monte Carlo simulation of the

accelerator and beam delivery complex that is capable of tracking individual electrons through the accelerator and transport line up to the Hall D tagger. Electrons were injected into the simulation with a Gaussian phase-space distribution, but as they were tracked through the accelerator, some particles diffused far from the core of the beam and eventually formed an extended tail that appeared superimposed on top of the central normal distribution. The reason the halo formed is that, once a particle wandered outside the core, perhaps because of energy loss from synchrotron radiation or small-angle scattering from residual gas in the beam pipe, it began to sample magnetic fields in the lattice elements outside their linear region. This caused halo particles to continually accumulate deviations from the nominal orbit, and eventually to be lost by collisions with the walls of the vacuum chamber. As soon as a particle reached the inner radius of the beam pipe in the simulation, it was considered lost and removed from the simulation. It is the competition between processes that generate new halo particles and their eventual loss that determines the amount of halo seen at any point along the beam line.

Besides synchrotron radiation and beam-gas scattering, other processes feeding the halo include displaced or mis-powered magnets, mismatched optics, and intrabunch scattering. All of these effects are taken into account together in the simulation by introducing random errors in the alignment and field parameters of magnetic elements in the lattice, which result in displacements of the main beam from the nominal orbit within certain predefined envelopes. These perturbations are not large enough to degrade the quality of the central part of the beam, but they contribute to the growth of the halo in the way described above. Ref. [2] reports halo distributions for simulations with a 3 mm orbit perturbation envelope, a 6 mm envelope, and a 10 mm envelope. The recommendation of the authors was to consider the 3 mm envelope as a realistic design goal for the 12 GeV beam.

1 halo model extraction

In Ref. [2], the beam halo is defined as the fractional integral of the beam current that lies outside the central peak in the x or y projection of the transverse beam intensity profile. The region of the central peak is defined by ± 5.10 mm in x and ± 3.15 mm in y of the beam centroid. Each of the three simulation data sets presented contain 10^8 beam particles, of which over 95% reach the Hall D radiator. The x and y projections of the impact

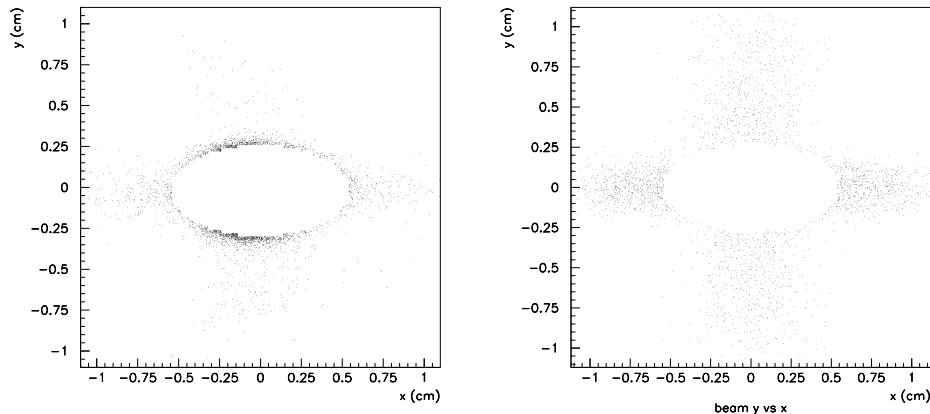


Figure 1: Caption goes here.

points on the transverse plane at the radiator position are plotted in Fig. 6 and fitted to the sum of a central Gaussian and a second-order polynomial halo parameterization. The parameters resulting from the fits are given in Tables 2-5.

One difficulty with extracting a halo model from these plots is that there is no unique way to convert a pair of x and y projections into a two-dimensional halo intensity distribution $h(x, y)$. Upon request, the authors were able to provide some two-dimensional histograms that showed the $x, y, x, \theta_x, y, \theta_y$, and θ_x, θ_y distributions for the 3 mm perturbation envelope simulation. These are shown in the first panels of Figs. 1-3. In order to make the halo events visible in these plots, it was necessary to mask off the areas of the plot inside the central 5σ region of the beam. In spite of the limited statistics of the halo events, after applying these masks it was possible to discern the main features of the halo distribution and extract a plausible analytical approximation to the phase-space density. The second panels in Figs. 1-3 show 1000 points each, generated according to the analytical model using Monte Carlo techniques.

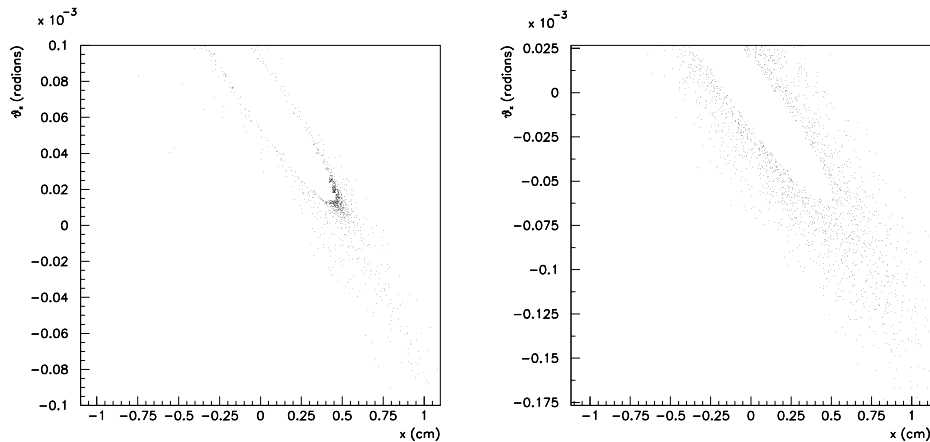


Figure 2: Caption goes here.

1.1 beam tails

Transverse emittance reflects the r.m.s. widths of the transverse position and angle distributions of electrons in the beam. These distributions follow a Gaussian profile, typically over several orders of magnitude. Beyond some radius, however, the distribution begins to fall more slowly than the Gaussian profile or even becomes relatively flat. These tails (or halo) contain relatively few particles relative to the central core of the beam, but can be important because they can interact with the dense materials surrounding the beam line and target and produce background. In the case of GlueX, the distance of order 100 m from the electron beam to the target (with the photon collimator in between) prevents such off-axis electrons from producing background in the GlueX detector. The same is not true of the tagging counters, however.

Photons produced by halo electrons have essentially zero chance of getting through the photon collimator. The reason for this is that they are produced by bremsstrahlung in materials that are orders of magnitude thicker than the crystal radiator, otherwise their photon yield would be negligible by reason of the low intensity of halo electrons relative to the core of the beam. Electrons passing through such a thick radiator undergo so much multiple scattering that the photon spot that they produce projected out to the distance of the collimator plane is orders of magnitude larger than the collimator aperture.

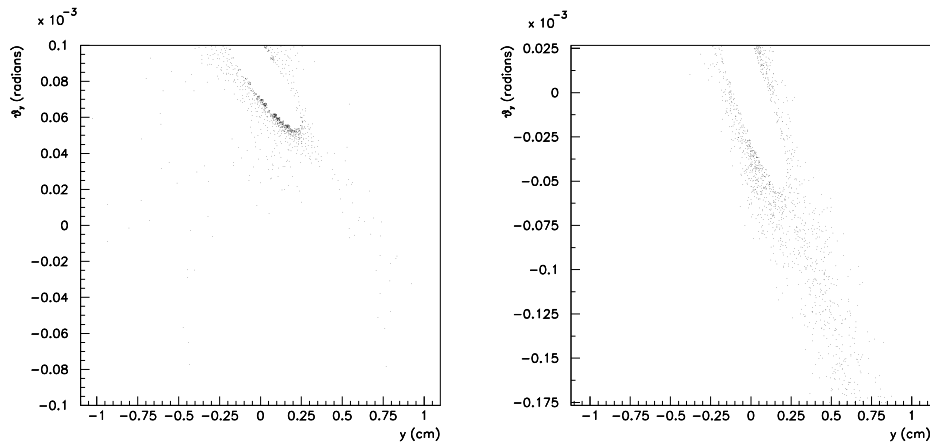


Figure 3: Caption goes here.

By contrast, the probabilities are somewhat higher that the degraded halo electron might find its way into one of the tagging counters. Beam particles which create hits in the tagging counters but no corresponding photon in the photon beam inflate the tagging efficiency. To make a quantitative estimate of this effect a model is needed for the distribution of materials in the vicinity of the beam axis upstream of the tagger and a spatial and momentum distribution for the halo particles.

A zeroth-order estimate for a safe upper limit for beam halo intensity is obtained as follows. Fit the transverse beam position distribution to a Gaussian function and subtract this distribution from the full beam population. The remaining particles, described as the halo population, are spread out over a relatively large spot compared to the original Gaussian radius. Assume that all of the halo beam particles end up striking some vacuum, support or magnetic element on their way through the tagger and that they all either scatter into a tagging counter themselves or produce secondaries that do. Under these assumptions, one may ask what fraction of the original beam may belong to the halo population without degrading the tagging efficiency by more than 1%. Under these somewhat perverse assumptions, the upper limit on the halo integral is 10^{-6} .

If this halo level were easy to guarantee coming from CEBAF at 12 GeV then our work would be done. However we have been assured that it is

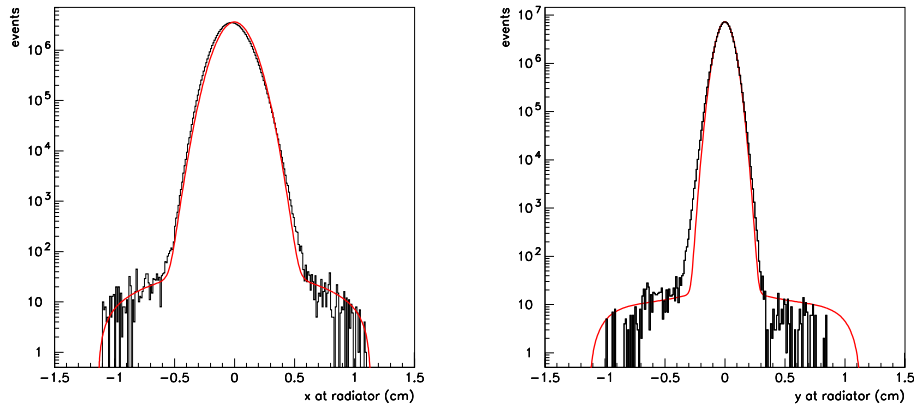


Figure 4: Caption goes here.

not. To make progress in refining this estimate, more information regarding the distribution of materials around the beam and the halo phase space distribution is needed. Experience with CEBAF at 6 GeV has shown that the latter can be difficult to predict and sometimes to control. On the other hand, we can configure the beamline elements to minimize the amount of material in the region upstream of the tagger which may cause the electron beam tails to scrape and produce background in the tagging counters. The following preliminary description of the region surrounding the beam in the region of the radiator has been studied using a GlueX tagger Monte Carlo simulation.

- A square aluminum frame with an inner cutout region of dimensions $1.5 \times 1.5 \text{ cm}^2$, outer dimensions $3 \times 3 \text{ cm}^2$ and thickness 3 mm.
- A stainless steel beam pipe leading through the tagger quadrupole from the radiator housing to the tagger vacuum box of outer diameter 3.8 cm and thickness 1.5 mm.
- A pressure of 10^{-4} Torr in the tagger vacuum.
- A 3 cm gap between the poles of the tagger dipoles.

In order to estimate the background in the tagging spectrometer, particles were generated uniformly in a disk of radius 2.5 cm at the position of the Hall

D radiator. This is a very pessimistic model for what might emerge from a 1.5 inch beam pipe coming from the tunnel, so the results can be taken as a conservative estimate for the expected halo rates in the tagger.

Using this model, 10^6 halo events were tracked through the tagger geometry with magnetic field simulation and full shower generation. Fig. 7 shows the transverse profile at the position of the radiator of all electrons in this sample which produced hits in the tagging counters. The second panel in the figure is provided to help with interpreting the hit pattern. The central red square in the second panel is the diamond radiator. The crystal mounting frame is shown by a light blue rectangular outline around the crystal. Next in order of increasing radius is the entrance flange to the tagging spectrometer vacuum box (purple ring) whose inner diameter is equal to the gap between the poles of 3 cm, somewhat smaller than the 3.5 cm ID pipe leading into it (solid blue ring). The green horizontal structures at the top and bottom of the figure are the pole shoes of the first spectrometer dipole. Surrounding the beam pipe with a gap of a few mm is the spectrometer quadrupole (solid yellow) which is represented in the model as a large block of iron with a circular hole cut out of the middle. Clearly visible in the hit pattern are the outlines of the radiator crystal holder and the vacuum chamber entrance flange, while the beam pipe material and the quadrupole and dipole magnets appear as partial voids because they act as absorbers rather than sources of background events.

Fig. 7 shows that the entrance flange to the vacuum box is the largest single source of tagger backgrounds in the present simulation geometry. This conclusion may change, however, when the halo distribution is improved beyond the crude model of a uniform disk extending out to 2.5 cm in radius. For the purposes of an initial estimate, the current model is sufficient. of expected to reduce the background rates by a factor of 3-5 in

In this sample a total of 9480 hits were observed leaving energy more than 200 keV in the tagging microscope counters. One million beam particles represents 50 ns of real time under full-intensity running conditions of 10^8 tagged γ/s on the GlueX target. Hence if 10^{-5} of the total electron beam population were in the halo then the halo rate in the tagging counters would be 10k per 5 ms or 2 MHz, which corresponds to a inflation factor of 1% in the tagging efficiency. From this it follows that an upper bound of 10^{-5} on the halo fraction is sufficient to insure that its effect on the tagging efficiency is negligible. The only part of the halo that contributes significantly to the background in the tagging counters is what lies between the radii of 1.0 and

1.5 cm.

In addition to the tagger microscope counters, there is also an second array of tagging counters which covers a much broader range in photon beam energy is more coarsely segmented. This broad-band array is not used for tagging during polarized photon running, but it is extremely important for monitoring the quality and stability of the photon beam. It is also needed to align the crystal at the beginning of each run period. The simulation showed that a 10^{-5} halo creates a hit rate below 1% of the tagged photon rate across most of the counters, with the exception of the very low-energy electron end of the spectrum. The broad-band array extends up to 95% of the bremsstrahlung end-point, which means that it sees electrons of only 600 MeV energy at the extreme end. This end of the array is also the closest to the radiator, which means that the solid angle of these counters relative to sources in the radiator region is the greatest in the same place where the bremsstrahlung spectral intensity is at its minimum. Fig. 8 shows the fraction of the total hits in each of the counters in the broad-band array that would be generated by a halo with a beam fraction of 10^{-5} . Maintaining a 1% upper bound on the halo contribution to the count rate in the tagger at the high-energy photon end of the broad-band array would push the requirement on the total halo fraction down to 10^{-6} .

References

- [1] R.T. Jones, “GlueX Requirements for 12 GeV Electron Beam Properties”, GlueX-doc-645 (2006).
- [2] Y. Roblin and A. Freyberger, “Studies of Beam Halo Formation in the 12 GeV CEBAF Design”, JLAB-TN-06-048 (2006).

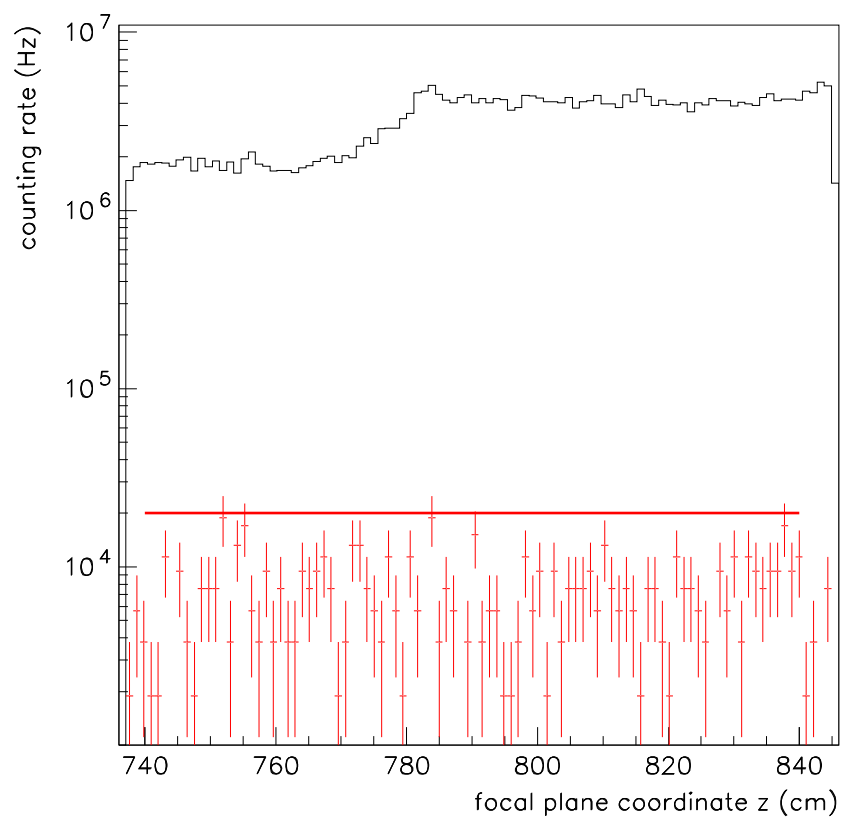


Figure 5: Caption goes here.

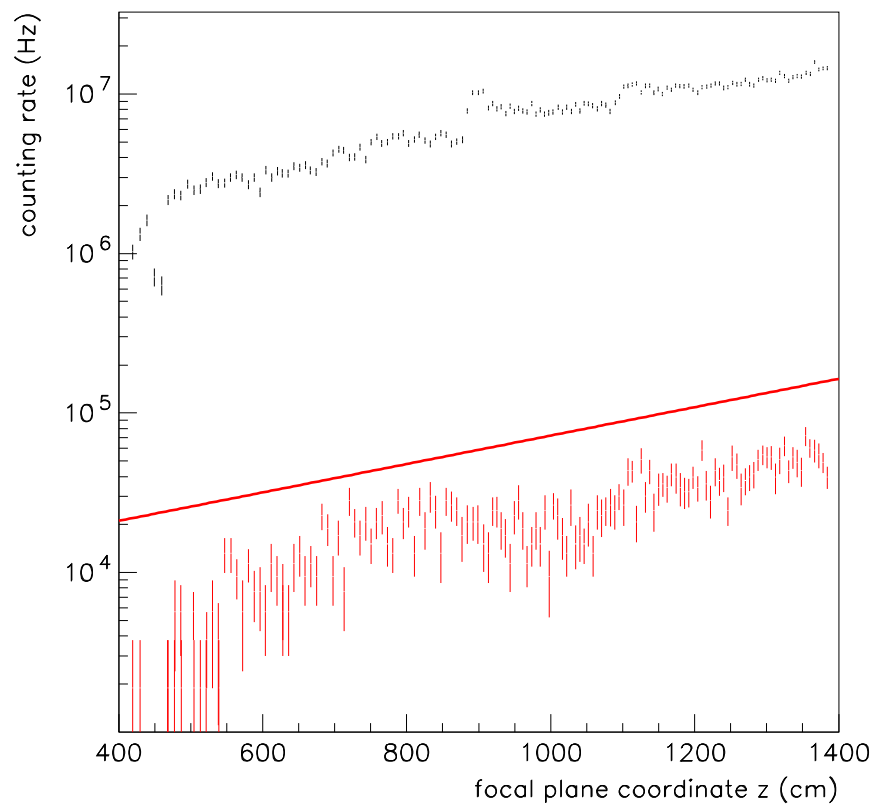


Figure 6: Caption goes here.

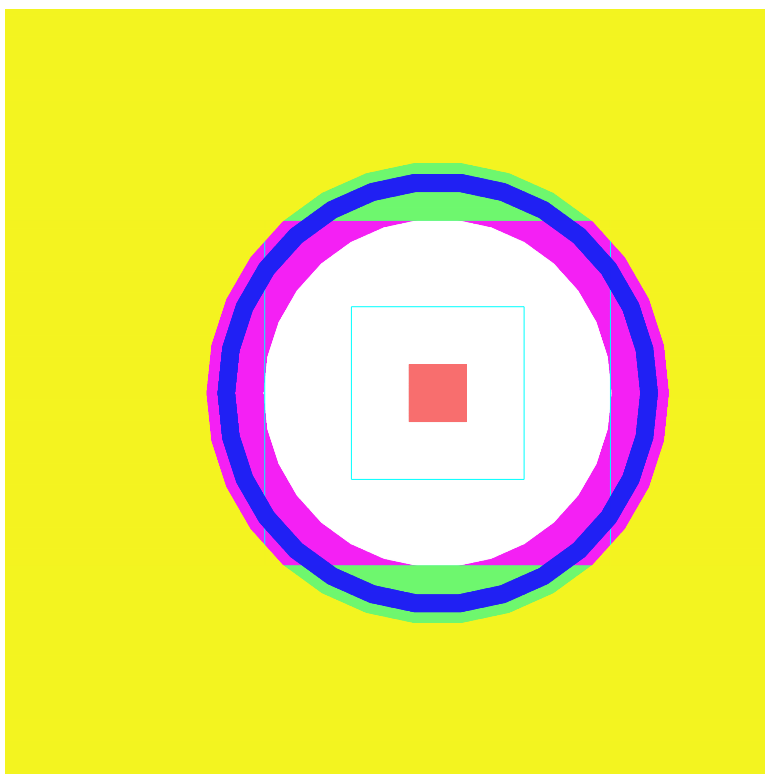
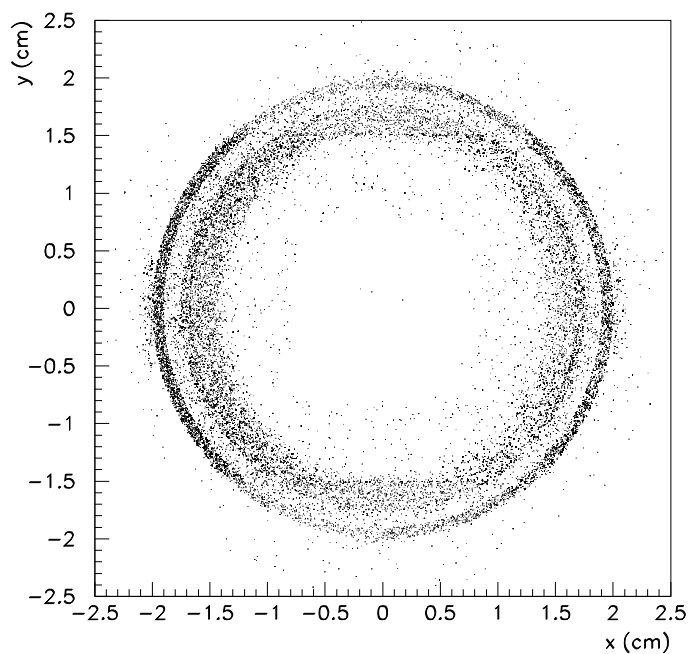


Figure 7: Transverse profile (top frame) at the radiator of particles in the beam halo that went on to create hits in the tagging counters. Each point is the intersection of an electron track with the plane containing the radiator. The hit pattern reflects the material distribution (bottom frame) as seen by the incoming electron beam. The two panels have matching dimensions. See text for details of the material map.

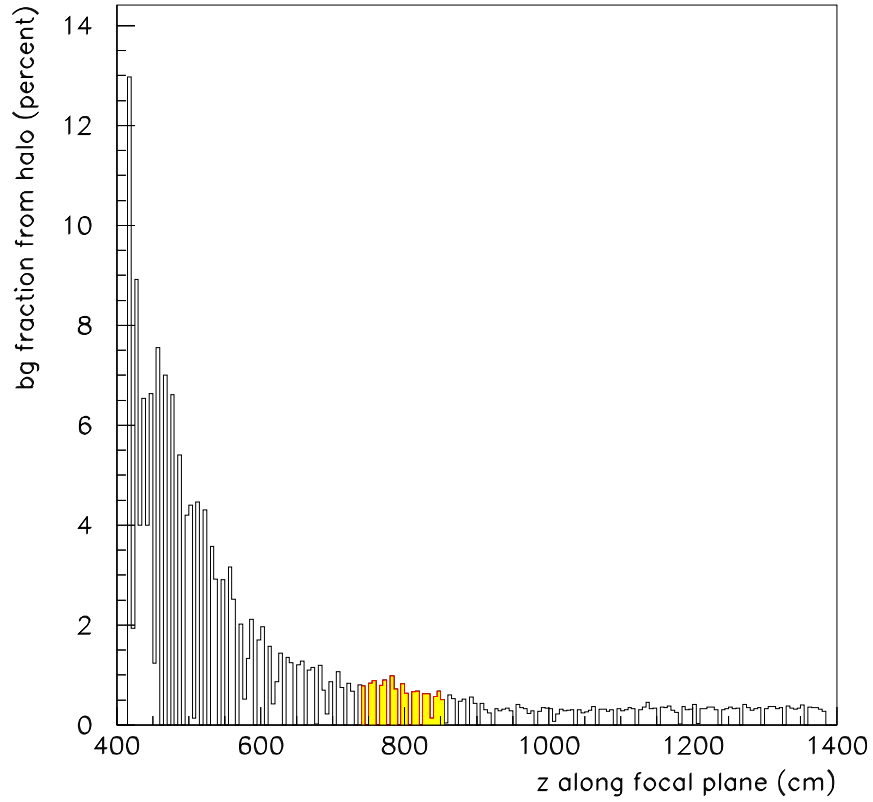


Figure 8: Percentage of hits in the broad-band tagging counters that are generated from electron beam halo particles, assuming a beam halo fraction of 10^{-5} . The electron beam energy scale is roughly linear in the z coordinate, varying from 600 MeV at the left end of the plot to 9 GeV at the right. The shaded region indicates the coverage of the microscope.